# ORIGINAL RESEARCH

Aryl Hydrocarbon Receptor Activity in Hepatocytes Sensitizes to Hyperacute Acetaminophen-Induced Hepatotoxicity in Mice

Fenja A. Schuran,[1] Christoph Lommetz,[1] Andreas Steudter,[1] Ahmed Ghallab,[2,3]
Björn Wieschendorf,[1] Dorothee Schwinge,[1] Sebastian Zuehlke,[4] Joerg Reinders,[2]
Joerg Heeren,[5] Ansgar W. Lohse,[1] Christoph Schramm,[1,6] Johannes Herkel,[1] and
Antonella Carambia[1]

[1]Department of Medicine I, University Medical Center Hamburg-Eppendorf, Hamburg, Germany; [2]Leibniz Research Centre for Working Environment and Human Factors, Technical University Dortmund, Dortmund, Germany; [3]Department of Forensic Medicine and Toxicology, Faculty of Veterinary Medicine, South Valley University, Qena, Egypt; [4]Center for Mass Spectrometry, Faculty of Chemistry and Chemical Biology, Technical University Dortmund, Dortmund, Germany; [5]Department of Biochemistry, University Medical Center Hamburg-Eppendorf, Hamburg, Germany; and [6]Martin Zeitz Center for Rare Diseases, University Medical Center Hamburg-Eppendorf, Hamburg, Germany
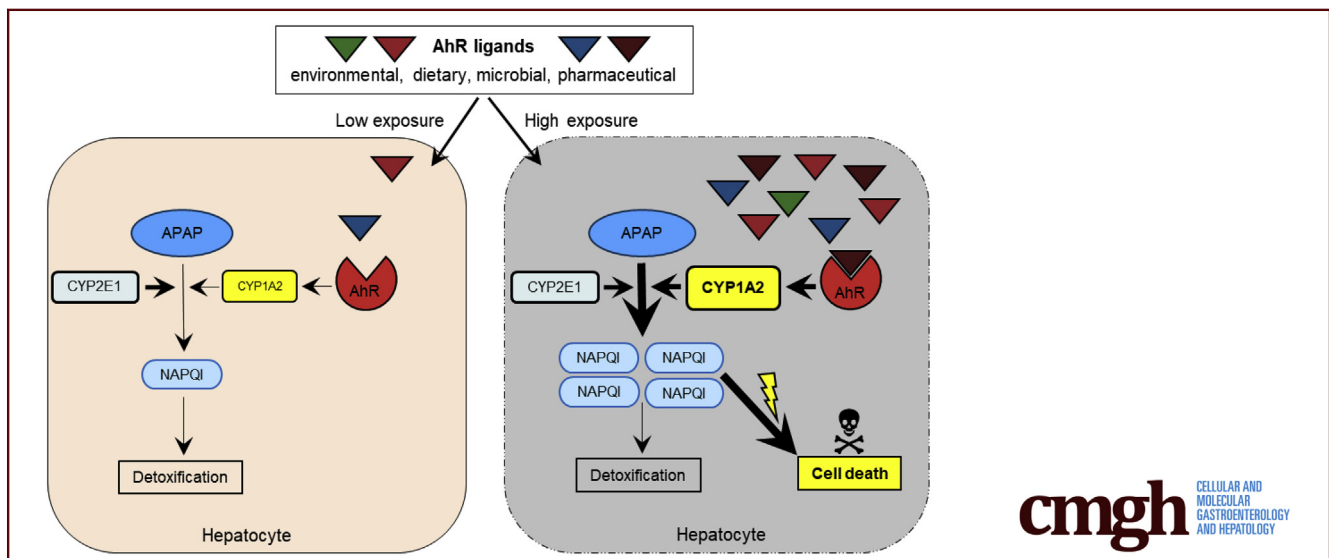
SUMMARY

Acetaminophen can induce liver injury with variable clinical outcome. We show that acetaminophen-induced hepatotoxicity is potentiated by activation of the transcription factor aryl hydrocarbon receptor (Ahr). Therefore, varying exposition to activating Ahr ligands might explain individual sensitivity to acetaminophen.

BACKGROUND & AIMS: Acetaminophen (APAP)-induced liver injury is one of the most common causes of acute liver failure, however, a clear definition of sensitizing risk factors is lacking. Here, we investigated the role of the ligand-activated transcription factor aryl hydrocarbon receptor (Ahr) in APAP-induced liver injury. We hypothesized that Ahr, which integrates environmental, dietary, microbial and metabolic signals into complex cellular transcriptional programs, might act as a rheostat for APAP-toxicity.

METHODS: Wildtype or conditional Ahr knockout mice lacking Ahr in hepatocytes (Alb$^{\Delta/\Delta Ahr}$) or myeloid cells (LysM$^{\Delta/\Delta Ahr}$) were treated with the specific Ahr ligand 2-(1'H-indole-3'-carbonyl)-thiazole-4-carboxylic acid methyl ester (ITE) together with APAP.

RESULTS: Ahr activation by ITE, which by itself was non-toxic, exacerbated APAP-induced hepatotoxicity compared to vehicle-treated controls, causing 80% vs. 0% mortality after administration of a normally sublethal APAP overdose. Of note, Ahr activation induced hepatocyte death even at APAP doses within the therapeutic range. Aggravated liver injury was associated with significant neutrophil infiltration; however, lack of Ahr in myeloid cells did not protect LysM$^{\Delta/\Delta Ahr}$ mice from exacerbated APAP hepatotoxicity. In contrast, Alb$^{\Delta/\Delta Ahr}$ mice were largely protected from ITE-induced aggravated liver damage, indicating that Ahr activation in hepatocytes, but not in myeloid cells, was instrumental for disease exacerbation. Mechanistically, Ahr activation fueled hepatic accumulation of toxic APAP

metabolites by up-regulating expression of the APAP-metabolizing enzyme Cyp1a2, a direct Ahr downstream target.

CONCLUSIONS: Ahr activation in hepatocytes potentiates APAP-induced hepatotoxicity. Thus, individual exposition to environmental Ahr ligands might explain individual sensitivity to hyperacute liver failure. *(Cell Mol Gastroenterol Hepatol 2021;11:371–388; https://doi.org/10.1016/j.jcmgh.2020.09.002)*

Keywords: APAP; Acute Liver Failure; Ahr; Cyp1a2.

Acetaminophen (APAP), also known as or paracetamol, is one of the most commonly used analgesic and antipyretic drugs worldwide.[1] In the United States, APAP toxicity is the most frequent cause of drug-induced liver injury and acute liver failure, accounting for more than 20% of liver transplantations.[1] Whereas about 90% of APAP is normally degraded into nontoxic metabolites and eliminated via the urine, about 10% is transformed into the highly reactive metabolite NAPQI (N-acetyl-para-benzo-quinone imine), mainly by hepatic cytochrome CYP2E1, but also by additional enzymes such as CYP1A2.[2] NAPQI strongly interferes with mitochondrial function, necessitating its rapid detoxification by glutathione (GSH) via formation of nontoxic cysteine conjugates.[1] Although adverse reactions to APAP usually occur only upon intentional or unintentional ingestion of an APAP overdose, there is increasing evidence that also therapeutic APAP doses can provoke toxic liver injury in some individuals.[1,3–5] However, the risk factors that sensitize individuals to APAP toxicity are not clear.[6]

The aryl hydrocarbon receptor (Ahr) is a ubiquitously expressed transcription factor that was initially described as the dioxin receptor, promoting toxic effects such as teratogenesis or tumor development when activated by the exogenous compound TCDD (2,3,7,8-tetrachlorodibenzo-p-dioxin).[7] However, it has become clear that many Ahr ligands are nontoxic dietary or microbial derived metabolites with potent immunomodulatory function.[8,9] Of note, it has been recently shown that microbiota-derived Ahr ligands can modulate inflammatory responses in the liver and are depleted in mice fed a high-fat diet.[10] Thus, the abundance of nontoxic Ahr ligands in an individual can depend on diet or microbiota composition.

Recent studies suggested a link between individual sensitivity to APAP and alterations in the gut microbiota and their metabolites.[11,12] Given that Ahr senses various dietary and microbial derived metabolites, we hypothesized that individual APAP sensitivity might be influenced by Ahr activation. This notion is supported by the observation that the Chinese medical herb *Polygonum multiflorum* Thunb, and its main active compound 2,3,4′,5-tetrahydroxystilbene-2-O-β-D-glucoside, which nonselectively activates Ahr but also other transcription factors, seems to promote APAP hepatotoxicity.[13] By the same token, it was shown that the increased sensitivity to APAP of mice with liver-specific miRNA-122 knockout seemed to correlate with upregulation of Ahr, Cyp1a2, and Cyp2e1.[14] Of note, Ahr activation

directly induces expression of Cyp1a2,[15] which can metabolize APAP to toxic NAPQI.[1] Although it is believed that Cyp2e1 is the key enzyme involved in the formation of toxic APAP metabolites,[1] Cyp1a2 seems to be of relevance, as only *Cyp2e1* and *Cyp1a2* double knockout mice are completely protected from APAP-induced liver injury.[2]

To test the hypothesis that Ahr activation might influence APAP toxicity, we subjected mice to a combined treatment with APAP and the nontoxic Ahr-activating ligands ITE (2-(1′H-indole-3′-carbonyl)-thiazole-4-carboxylic acid methyl ester) or FICZ (6-formylindolo[3,2-b]-carbazole), which proved to have beneficial immunomodulatory effects in various preclinical models of autoimmune diseases.[9,16] We found that APAP-induced liver injury was strongly exacerbated by Ahr activation. Of note, severe liver injury was induced by co-administration of ITE even at APAP doses that are equivalent to Food and Drug Administration–approved human doses considered as safe ($\leq$4000 mg/d).[1] The observed devastating effect of Ahr activation was linked to the upregulation of Cyp1a2, promoting the synthesis of toxic APAP metabolites. Using conditional *Ahr* knock-out mice, we demonstrated that ITE-induced disease exacerbation depended on Ahr activity in hepatocytes, not in myeloid cells.

These findings suggest that increased exposure to Ahr ligands deriving from different sources might fuel accumulation of toxic APAP metabolites and explain hypersensitivity to APAP observed in some individuals. In conclusion, our study should prompt a greater awareness of potentially adverse interactions between APAP and nontoxic Ahr ligands.

Results

Ahr Activation by ITE Induces Hyperacute APAP Hepatotoxicity

To assess the role of Ahr activation in APAP-induced liver injury, wild-type mice were treated with ITE twice before injection of a normally sublethal dose of APAP (350 mg/kg). Strikingly, ITE pretreatment led to a significant exacerbation of APAP hepatotoxicity, as indicated by a deteriorated body condition compared with vehicle pretreated control mice over the course of the experiment (*P* < .0001) (Figure 1*A*). Even more strikingly, ITE pretreatment provoked a highly unusual death rate of 80% within the first 8 hours post-APAP treatment (*P* = .0002) (Figure 1*B*), whereas all control mice receiving vehicle before APAP injection or no APAP (vehicle or ITE only) survived. Transaminase levels measured in sera as early as 4 hours post-APAP treatment confirmed strongly increased

liver damage in mice receiving combined ITE and APAP treatment as compared with vehicle and APAP treatment (alanine aminotransferase [ALT], $P < .001$ [Figure 1C]; aspartate aminotransferase [AST], $P < .0001$ [Figure 1D]). Accordingly, hematoxylin and eosin (H&E) (Figure 1E),

terminal deoxynucleotidyl transferase-mediated dUTP nick end labelling (TUNEL) ($P < .001$) (Figure 1F and G), and cleaved caspase-3 ($P < .001$) (Figure 1H and I) stainings of livers from mice treated with ITE and APAP revealed vast areas of hepatocellular death that were composed of only
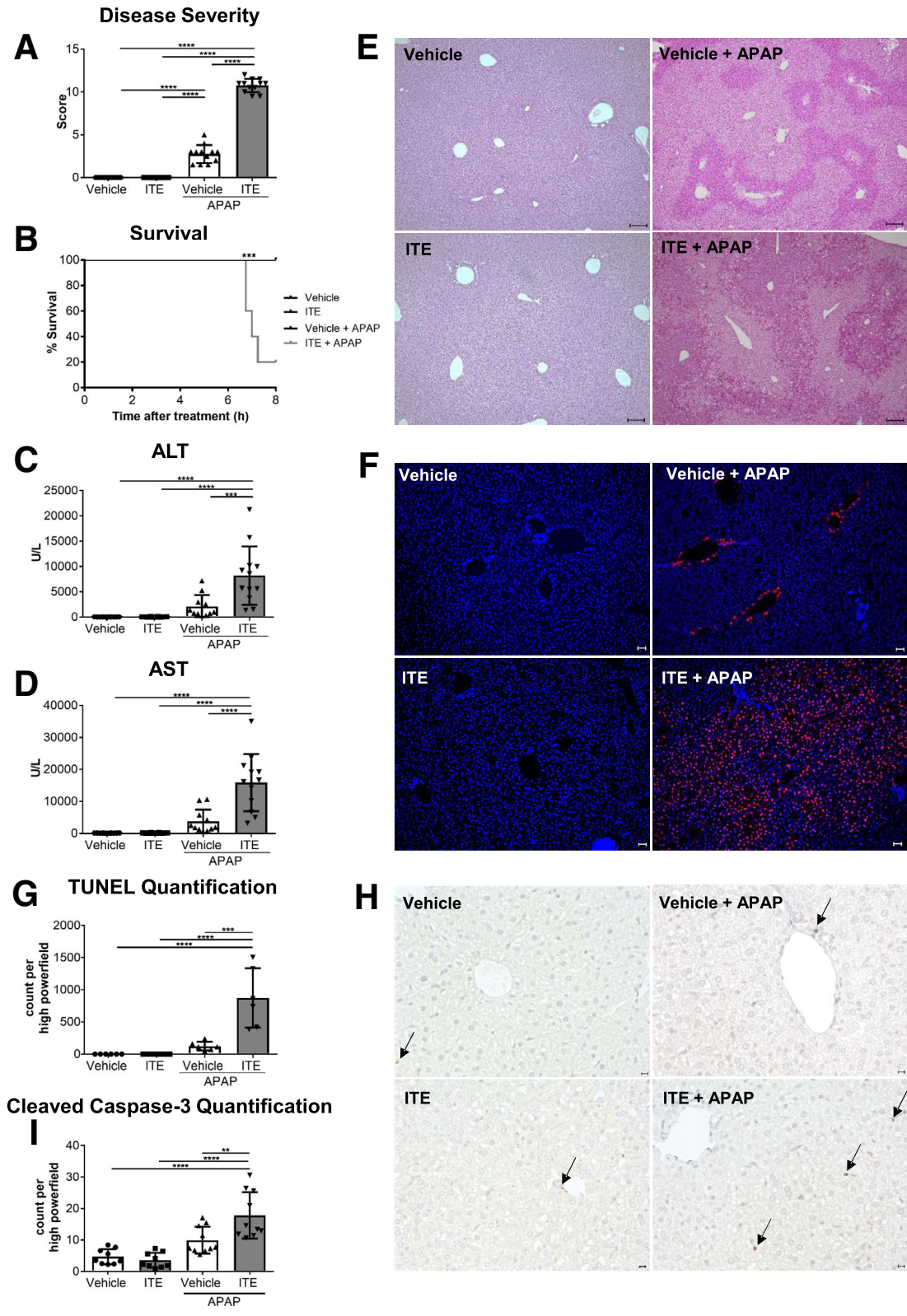
few apoptotic and mainly necrotic cells. In contrast to control livers, these areas were not confined to central veins.

Of note, we did not observe any signs of liver injury upon ITE treatment alone without APAP intoxication (Figure 1). Thus, activation of Ahr by the nontoxic ligand ITE did not produce adverse effects when given alone, but significantly exacerbated APAP-induced liver injury.

Ahr Activation Promotes Accumulation of Toxic Acetaminophen Metabolites

To further elucidate the mechanisms behind the observed hyperacute APAP hepatotoxicity induced by Ahr activation, we first quantified hepatic RNA expression of Ahr and the major APAP metabolizing enzymes Cyp1a2 and Cyp2e1. Expression of all 3 genes was significantly upregulated in ITE- and APAP-treated mice, as compared with vehicle-treated control mice (Ahr: $P = .0187$ [Figure 2A]; Cyp1a2: $P < .0001$ [Figure 2B]; Cyp2e1: $P = .0077$ [Figure 2C]). At the protein level, Cyp1a2, but not Cyp2e1, was significantly elevated upon combined ITE and APAP treatment, as assessed by immunofluorescence staining (Figure 2D) as well as immunoblotting (Figure 2E and F). Of note, expression of the direct Ahr target gene Cyp1a2 was also upregulated when ITE was administered alone without APAP (Figure 2B, E, F), in contrast to Cyp2e1, which is not a direct downstream target of Ahr. In line with these observations, total GSH levels were significantly lower in ITE-treated mice following APAP intoxication as compared with vehicle control mice ($P = .0005$) (Figure 2G). As a consequence, Ahr activation by ITE led to significantly increased accumulation of APAP adducts, reflecting toxic NAPQI formation (APAP-GSH: $P < .0001$, APAP-CYS: $P = .0010$, APAP-NAC: $P = .0006$) (Figure 2H). Thus, ITE pretreatment seemed to aggravate APAP-induced liver injury by fueling generation of toxic APAP adducts via Cyp1a2.

Ahr-Mediated Hyperacute APAP Hepatotoxicity Is Associated With Increased Infiltration of Inflammatory Cells

Recently, it has been reported that the severity of APAP-induced liver injury is critically dependent on the infiltration of inflammatory monocytes and neutrophils.[17,18] Therefore, we next asked whether inflammatory monocytes were involved in the observed exacerbation of APAP-induced liver injury following Ahr activation by ITE pretreatment. In fact, we observed upregulation of inflammatory monocyte and neutrophil markers Itgam (CD11b), Ly6c1, and Ly6g in the livers of mice treated with ITE and APAP as compared with control mice treated with vehicle and APAP (each $P = .0022$) (Figure 3A). Accordingly, flow cytometry confirmed increased hepatic accumulation of CD11b+ cells ($P = .0043$) (Figure 3D and E) of which the majority were Ly6C^{int}LY6G^{hi} neutrophils ($P = .0043$) (Figure 3B). However, CD11b+LY6C^{hi} inflammatory monocytes were not elevated as compared with control mice ($P = .3983$) (Figure 3B). Corresponding to the increased neutrophil infiltration, we found significantly elevated levels of the chemokine Ccl2 ($P = .0022$) (Figure 3C) as well as increased expression of the inflammatory cytokines Il6, Tnf, Il18, and Il1b (each $P = .0022$) (Figure 3D). Of note, control mice receiving vehicle or ITE alone without additional APAP intoxication did not show any signs of liver inflammation neither on the cellular nor on the molecular level (Figure 3). In conclusion, these data show that exacerbation of APAP-induced liver injury following Ahr activation by ITE was associated with enhanced hepatic infiltration of inflammatory cells, the majority of which were neutrophils, and an increased inflammatory response.

## ITE-Mediated Ahr Activation in Myeloid Cells Does Not Aggravate Acetaminophen-Induced Liver Injury

As Ahr is a ubiquitously expressed transcription factor, it is constitutively expressed in hepatocytes[19] and myeloid cells,[20] including neutrophils. As all these cell types are involved in APAP-mediated liver damage, we sought to further dissect at the cellular level, how Ahr activation contributed to APAP-induced liver damage. To that end, we made use of conditional Ahr knockout mice lacking Ahr expression in myeloid cells (LysM$^{Δ/ΔAhr}$) including macrophages, monocytes, and granulocytes, as confirmed by quantitative polymerase chain reaction analysis of Ahr messenger RNA expression in isolated F4/80+ liver macrophages ($P = .0317$) (Figure 4A). Interestingly, we could not observe any differences in disease severity between LysM$^{Δ/ΔAhr}$ mice in comparison with their littermates when APAP was administered alone (ALT: $P = .5714$, AST: $P = .8983$) (Figure 4B). Moreover, when we subjected LysM$^{Δ/ΔAhr}$ mice and their littermates with functional Ahr to combined ITE and APAP treatment, disease severity between both

---

Figure 1. (*See previous page*). **Ahr activation by ITE induces hyperacute liver damage.** Female wild-type mice were treated with vehicle or ITE alone, or with vehicle + APAP or ITE+ APAP (n = 12 each). Samples were analyzed 4 hours post-APAP treatment and survival was monitored for 8 hours. (A) Disease score reflecting general condition, (B) survival curve, (C, D) serum liver transaminases, (E) H&E staining of liver tissue (scale bar = 100 μm), (F,G) hepatocyte damage assessed by TUNEL staining (red; nuclei are stained in blue) (scale bar = 50 μm), (H, I) apoptotic cells visualized by cleaved caspase-3 staining. Scale bar = 50 μm. Pictures were taken using a Biorevo Keyence BZ-9000 microscope with objective from Nikon (Plan Apo 10x/0,45 ∞/0.17 WD 4.0) and the Keyence BZ II Viewer and Analyzer software. Two pooled experiments of 3 independent experiments are shown. For statistical analysis, a 1-way analysis of variance followed by Tukey's multiple comparisons test was applied. For the survival curve, statistical significance was tested with the log-rank (Mantel-Cox test) and Gehan-Breslow-Wilcoxon test. Results are shown as mean ± SD. **$P < .01$, ***$P < .001$, ****$P < .0001$.

groups remained similar, as indicated by similar body condition ($P = .3853$) (Figure 4C) and serum transaminase levels (ALT: $P = .3874$; AST: $P = .7879$) (Figure 4D), similar liver histology (H&E, TUNEL, and cleaved caspase-3 staining) (Figure 4E–I), and similar infiltration of inflammatory monocytes and neutrophils (Itgam [integrin subunit alpha M]: $P = .4740$; Ly6c1: $P = .3874$; Ly6g: $P > .9999$) (Figure 4J). These findings suggest that Ahr activation by ITE in the myeloid compartment was not responsible for the observed aggravation of APAP-induced liver injury.
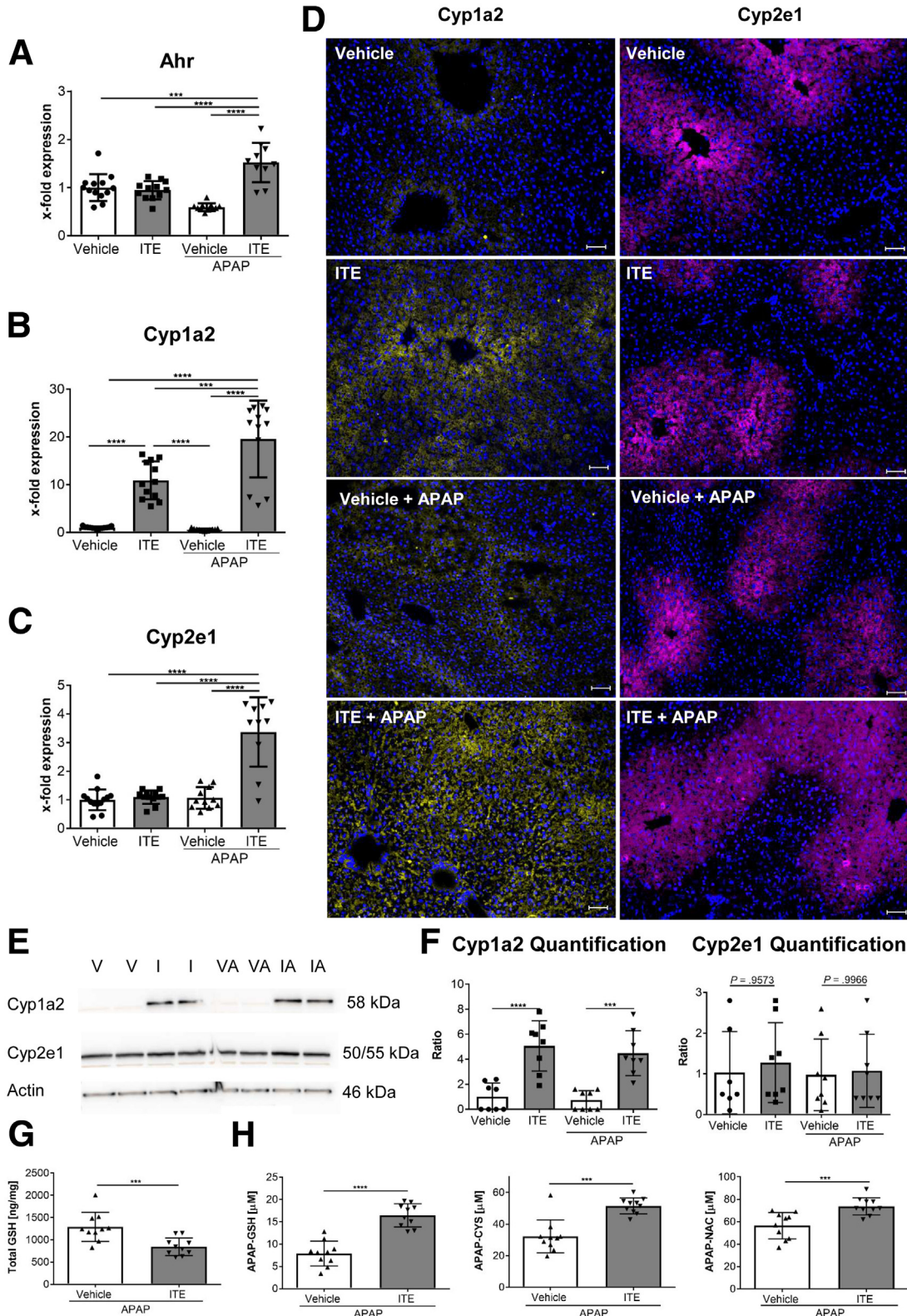
Ahr Activation in Hepatocytes Is Responsible for ITE-Mediated Induction of Hyperacute APAP Hepatotoxicity

We then made use of conditional *Ahr* knockout mice lacking *Ahr* expression in hepatocytes (Alb$^{\Delta/\Delta Ahr}$), as confirmed by quantitative polymerase chain reaction analysis ($P = .0007$) (Figure 5A). Liver damage upon APAP treatment was significantly reduced in Alb$^{\Delta/\Delta Ahr}$ mice lacking Ahr in hepatocytes compared with their littermates with functional Ahr (ALT: $P = .0298$, AST: $P = .0356$) (Figure 5B). Thus, already at baseline levels, activity of Ahr in hepatocytes seemed to aggravate APAP-induced liver injury. Interestingly, upon combined ITE and APAP treatment, Alb$^{\Delta/\Delta Ahr}$ mice were largely protected from disease exacerbation, as compared with their littermate control mice, indicating that activation of Ahr in hepatocytes was the major determinant for ITE-mediated aggravation of APAP-induced liver damage. Accordingly, the overall body condition of Alb$^{\Delta/\Delta Ahr}$ mice was significantly improved ($P < .0001$) (Figure 5C), and serum ALT ($P = .0012$) (Figure 5D) and AST ($P = .0002$) (Figure 5D) levels were significantly lower as compared with littermate control mice. Moreover, H&E, TUNEL, and cleaved caspase-3 staining of liver sections revealed greatly reduced hepatocyte damage in Alb$^{\Delta/\Delta Ahr}$ mice following combined APAP and ITE treatment (Figure 5E–I). Mechanistically, the protection from aggravated hepatotoxicity in Alb$^{\Delta/\Delta Ahr}$ mice was mainly linked to the significantly lower induction of Cyp1a2 ($P < .0001$) (Figure 6A), whereas Cyp2e1 ($P = .1639$) (Figure 6B) expression was only slightly reduced. These findings were confirmed at the protein level by immunofluorescence staining as well as immunoblotting of Cyp1a2 and Cyp2e1 (Figure 6C and D), indicating that the induction of Cyp1a2 and not Cyp2e1 seemed to be the main cause for the observed ITE-mediated aggravation of APAP toxicity. Correspondingly, protection from disease exacerbation in Alb$^{\Delta/\Delta Ahr}$ mice was associated with significantly higher GSH levels ($P = .0159$) (Figure 6E) as well as significantly decreased levels at least of the APAP-GSH adduct as compared with littermate control mice ($P = .0095$) (Figure 6F). Moreover, livers of Alb$^{\Delta/\Delta Ahr}$ mice showed a lower degree of inflammation, as indicated by diminished hepatic expression of the inflammatory cytokines *Il6* ($P = .0158$) (Figure 6G), *Il1b* ($P = .0021$) (Figure 6G), and *Tnf* ($P = .0150$) (Figure 6G).

Low-Dose APAP in Combination With ITE Is Sufficient to Induce Hepatocellular Damage

So far, we analyzed the role of Ahr activation in APAP-mediated hepatotoxicity induced by an overdose of 350 mg/kg, which is equivalent to 28.4 mg/kg in humans. In order to determine the impact of Ahr activation at lower, normally subclinical APAP doses within the therapeutic range, we next performed a dose escalation experiment in which wild-type mice were treated with 0, 50, 100, 205, or 350 mg/kg APAP corresponding to the human equivalent doses 0, 4.1, 8.1, 16.6, or 28.4 mg/kg (calculated according to Reagan-Shaw et al)[21] in combination with 200μg ITE or vehicle (Figure 7). Strikingly, already at a very low mouse dose of 50mg/kg APAP, which normally does not cause any signs of liver damage, ITE pretreatment induced considerable hepatocyte death as indicated by upregulation of ALT and AST serum levels (ALT: $P = .1255$ [Figure 7A]; AST: $P = .0173$ [Figure 7B]). At the mouse dosage of 205 mg/kg that is equivalent to the recommended maximum single dose of 1000 mg APAP in a human of 60kg weight,[1,21] additional ITE treatment significantly exacerbated APAP hepatotoxicity (ALT: $P = .0043$ [Figure 7A]; AST: $P = .0022$ [Figure 7B]). To confirm these findings, we performed TUNEL staining of the respective liver sections. As expected, the numbers of dead hepatocytes increased with escalating APAP doses. Moreover, at each APAP dose tested, livers of ITE-treated mice showed considerably more dead cells compared with vehicle control mice, even at low APAP doses within the therapeutic range (Figure 7C).

In order to assess whether sensitization to hyperacute APAP-induced liver damage correlates with the bioavailability of Ahr-activating ligands, we next performed an ITE dose escalation experiment. Interestingly, already upon application of low doses of ITE (ie, one-third or one-tenth of the published standard therapeutic dose),[22–24] hepatocellular damage was significantly increased, as shown by elevated serum transaminase levels (ALT: $P = .0022$ [Figure 7D]; AST: $P = .0022$ [Figure 7E]) and increased numbers of TUNEL-positive hepatocytes (Figure 7F). Thus, already at low levels, Ahr ligands can significantly aggravate APAP-mediated liver damage. Taken together, these findings support a possible clinical relevance of Ahr activation for the development of hyperacute APAP hepatotoxicity.

Ahr Activation by FICZ in Combination With APAP Induces Hyperacute Liver Damage

To confirm that exacerbation of APAP-induced hepatotoxicity was not a singular effect of ITE, but also of other Ahr ligands, we also tested APAP toxicity in combination with FICZ (Figure 8). Similar to ITE, FICZ greatly increased hepatotoxicity when given in combination with APAP, as

Figure 2. (*See previous page*). **Ahr activation promotes accumulation of toxic acetaminophen metabolites.** Female wild-type mice were treated with vehicle or ITE alone, or with vehicle + APAP or ITE + APAP (n = 12 each). Hepatic gene expression of (*A*) *Ahr*, (*B*) *Cyp1a2* and (*C*) *Cyp2e1* were analyzed 4 hours post-APAP treatment. Target gene expression is depicted as x- fold expression compared with the vehicle control. (*D*) Representative stainings of hepatic Cyp1a2 (yellow) and Cyp2e1 (purple) protein expression. Nuclei are stained in blue. Scale bar = 50 μm. Pictures were taken using a Biorevo Keyence BZ-9000 microscope with objective from Nikon (Plan Apo 10x/0,45 ∞/0.17 WD 4.0) and the Keyence BZ II Viewer and Analyzer software. (*E, F*) Western blot analysis of Cyp1a2 and Cyp2e1 protein expression (n = 8). (*G*) Total GSH levels in liver tissue and (*H*) toxic APAP adducts in plasma 30 min post APAP treatment (n = 10). Two pooled of 3 independent experiments are shown. For statistical analysis, a 1-way analysis of variance followed by Tukey's multiple comparisons test was used. Results are shown as mean ± SD. *$P < .05$, **$P < .01$, ***$P < .001$, ****$P < .0001$. I, ITE; IA, ITE + APAP; V, vehicle; VA, vehicle + APAP.
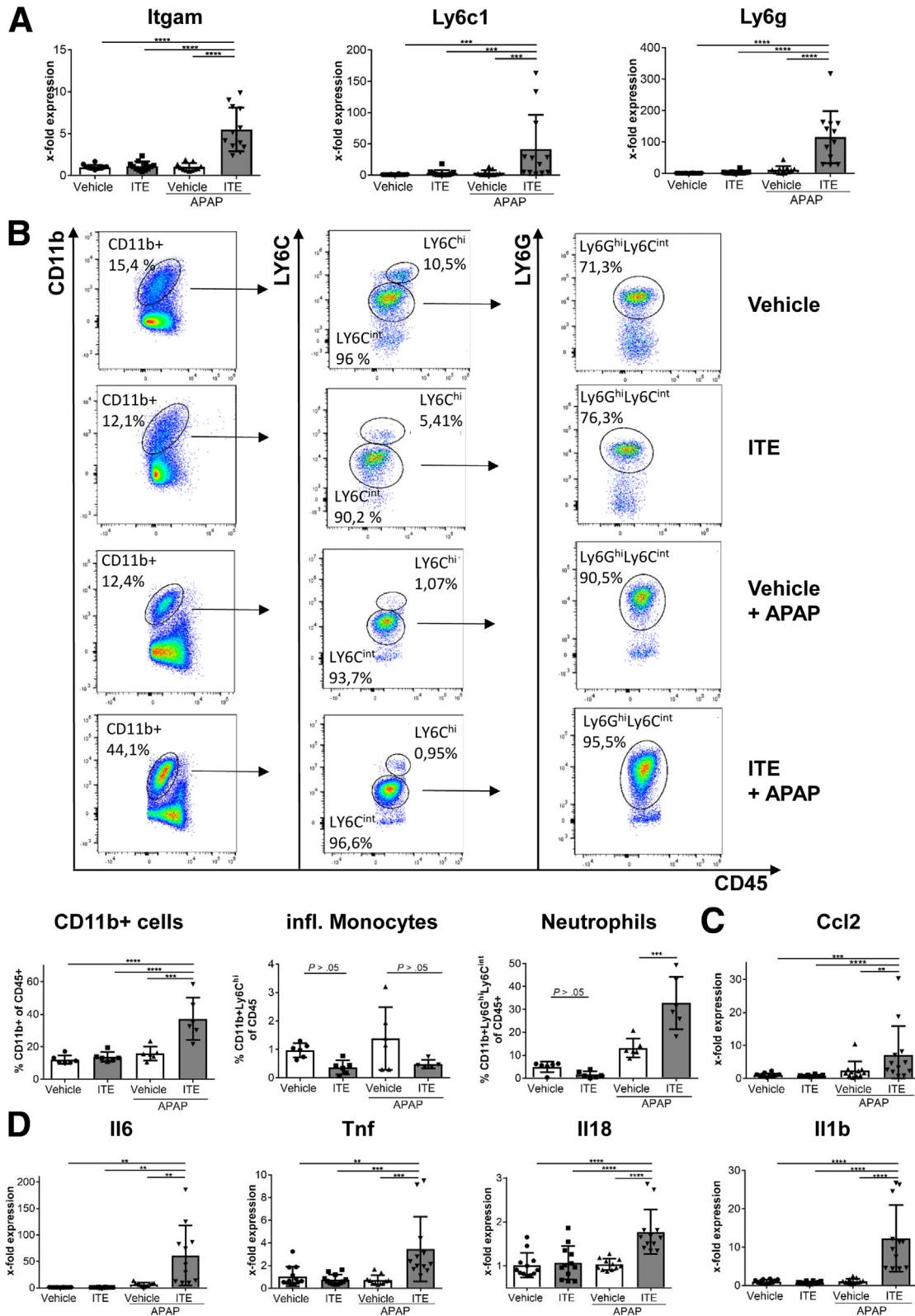
Figure 3. Ahr-mediated hyperacute APAP hepatotoxicity is associated with increased infiltration of inflammatory cells. Female wild-type mice were treated with vehicle or ITE alone, or with vehicle + APAP or ITE + APAP (n = 12 each) and analyzed 4h post-APAP treatment. (*A*) Hepatic gene expression of the monocyte and neutrophil markers *Itgam*, *Ly6c1*, and *Ly6g*. (*B*) Flow cytometric analysis of liver-infiltrating CD11b+ Ly6C^{hi} monocytes and CD11b+ Ly6G^{hi} Ly6C^{int} neutrophils (n = 6 each). (*C*) Hepatic gene expression of the inflammatory mediators *Ccl2*, *Il6*, *Tnf*, *Il18*, and *Il1b*. Two pooled experiments of 3 independent experiments are shown. Results are shown as mean ± SD. For statistical analysis, a 1-way analysis of variance followed by Tukey's multiple comparisons test was performed. *P < .05, **P < .01, ***P < .001, ****P < .0001.

indicated by aggravated body condition ($P < .0001$) (Figure 8A), upregulation of serum transaminases (ALT: $P = .0010$; AST: $P = .0017$) (Figure 8B) and increased hepatocellular death as assessed by H&E, TUNEL, and cleaved caspase-3 staining (Figure 8C–G). Moreover, FICZ-induced disease exacerbation was associated with hepatic upregulation of Ahr ($P = .0013$) (Figure 8H) and Cyp1a2 ($P < .0001$) (Figure 8I). Of note, hepatic Cyp2e1 expression in FICZ treated mice was similar to the control group ($P = .3730$) (Figure 8I), confirming that Cyp1a2 and not Cyp2e1
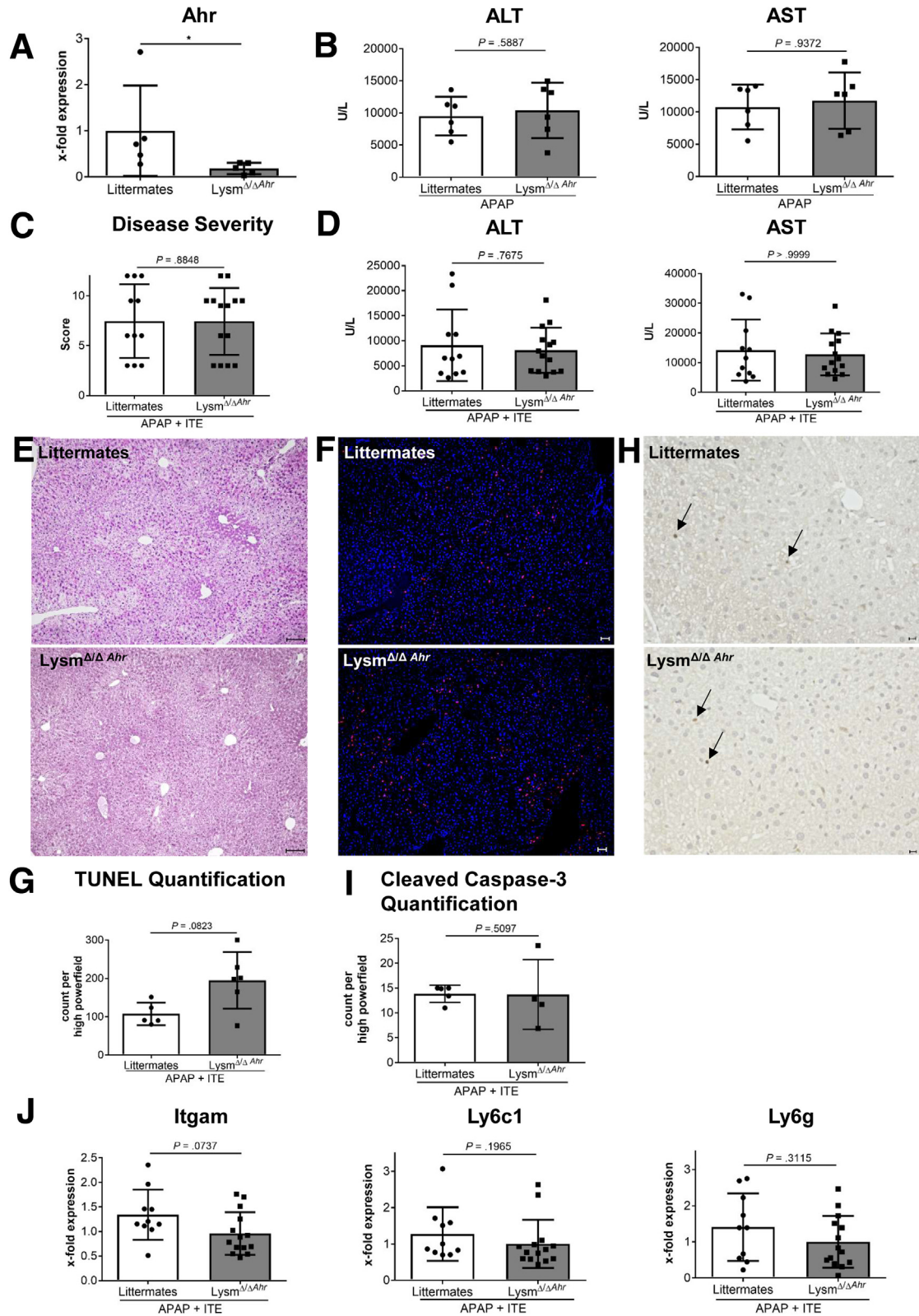
seems to be the main mediator of Ahr-dependent exacerbation of APAP-induced hepatotoxicity. These findings were further confirmed by Western blot analysis of Cyp1a2 and Cyp2e1 at the protein level (Cyp1a2: $P = .0383$; Cyp2e1: $P = .1793$) (Figure 8J and K). Moreover, as observed in mice receiving combined APAP and ITE treatment (Figure 2), the increased liver damage in mice treated with APAP and FICZ was associated with hepatic upregulation of inflammatory cytokines (Il6: $P = .0001$; Tnf: $P = .0006$; Il1b: $P < .0001$) (Figure 8L). Thus, Ahr activation by nontoxic ligands such as ITE or FICZ promotes APAP-induced hyperacute liver injury already at standard therapeutic doses.

Ahr Activity Aggravates APAP Hepatotoxicity in Both Sexes in Equal Measure

Finally, as sex differences in sensitivity to APAP have been described,[25] we wondered whether the observed hypersensitivity to APAP in response to Ahr activation was sex-dependent. In line with the literature,[25] male mice (Figure 9A–F) displayed increased disease severity upon APAP intoxication, as compared with female mice (Figure 9G–L), indicated by higher ALT and AST levels after vehicle + APAP treatment (ALT in male mice 2307 U/L vs 812 U/L in female mice; AST in male mice 3789 U/L vs 1452 U/L in female mice). However, comparing the response to ITE treatment in APAP hepatotoxicity, we found a similar devastating effect in both sexes, as indicated by a significant increase in disease severity, serum transaminases, and induction of the APAP-metabolizing enzymes Cyp1a2 and Cyp2e1 ($P = .0022$ [Figure 9A–C]; $P = .0152$ [Figure 9D]; $P = .0022$ [Figure 9E–I]; $P = .0043$ [Figure 9J–L]). Thus, the here described hyperacute APAP-induced hepatotoxicity in response to Ahr activation occurs to a similar degree in both sexes.

Discussion

Over the past years, an increasing number of new endogenous and exogenous Ahr ligands has been identified, which can originate from various sources such as endogenous metabolism, nutrition, or gut microbiota. Therefore, it can be assumed that everybody is constantly exposed to varying amounts of nontoxic Ahr ligands, depending on the individual's diet, metabolic status, or microbiota composition. Moreover, the potent immunosuppressive capacity of Ahr ligands such as FICZ, ITE, or I3C (indole-3-carbinol) metabolites[8,9] has been recognized and successfully tested as new drug candidates in preclinical mouse models of autoimmune or chronic inflammatory diseases, including models of psoriasis,[26] multiple sclerosis,[22] type 1 diabetes,[23] ulcerative colitis,[24] or food allergy.[27]

Given that APAP is one of the most common analgesic and antipyretic drugs, and that one of the major APAP-metabolizing enzymes, Cyp1a2, is directly induced by Ahr, we hypothesized that Ahr activating ligands might increase the formation of toxic APAP metabolites. Accordingly, Ahr activation by nontoxic ligands above a certain threshold might at least in part explain why individuals respond to APAP with different sensitivities.

Indeed, we found that combined treatment of mice with a sublethal dose of APAP and a therapeutic dose of ITE produced hyperacute APAP-induced liver injury (Figure 1). The aggravated phenotype was associated with increased liver infiltration mainly of neutrophils and increased expression of inflammatory cytokines (Figure 3). Even more importantly, combined ITE and APAP treatment significantly induced Cyp1a2 expression, promoting the formation of toxic APAP metabolites (Figure 2).

When we further dissected the respective contributions of Ahr activation by ITE in myeloid cells or hepatocytes to APAP-induced liver injury, we found Ahr activity in myeloid cells to be irrelevant, whereas Ahr activation in hepatocytes was crucial for disease exacerbation (Figures 4–6), as reflected by a significantly attenuated disease course in Alb$^{\Delta/\Delta Ahr}$ mice as compared with littermate control mice (Figure 5). Moreover, since the APAP-metabolizing enzyme Cyp1a2 is a direct downstream target of Ahr and is strongly induced by ITE, it is reasonable to assume that the production of bioactive APAP metabolites is enhanced by the combined APAP and ITE treatment. By the same token, the protection from aggravated liver damage upon APAP and ITE combination treatment observed in Alb$^{\Delta/\Delta Ahr}$ mice was mainly associated with the absence of Cyp1a2 induction, whereas Cyp2e1 expression was not affected (Figure 6). Thus, the Ahr-Cyp1a2 axis seems to be the major mechanistic link responsible for Ahr-dependent exacerbation of APAP-induced liver damage. These findings were confirmed with another Ahr ligand, FICZ, indicating that disease exacerbation caused by Ahr activation was not dependent on a particular activating ligand (Figure 8).

Figure 4. (*See previous page*). **ITE-mediated Ahr activation in myeloid cells does not aggravate acetaminophen-induced liver injury.** (*A*) Quantitative polymerase chain reaction–based verification of efficient Ahr knockdown in myeloid cells isolated from livers of female LysM$^{\Delta/\Delta Ahr}$ mice as compared with littermate control mice without Ahr deficiency in myeloid cells (n = 5 each). (*B*) Serum ALT and AST levels of female LysM$^{\Delta/\Delta Ahr}$ mice or their littermates 8 hours post APAP treatment (n = 6 each). (*C-J*) Male LysM$^{\Delta/\Delta Ahr}$ mice (n = 14) or littermate control mice (n = 11) were treated with ITE + APAP and analyzed 4h post-APAP treatment. We found no significant differences in (*C*) disease severity, (*D*) serum transaminase levels, (*E*) histological tissue damage (scale bar = 100 μm), (*F, G*) hepatocellular death as assessed by TUNEL staining (red; scale bar = 50 μm), (*H, I*) apoptosis as shown by cleaved caspase-3 analysis (scale bar = 50 μm), and (*J*) infiltration of inflammatory monocytes or neutrophils as assessed by gene expression levels of Itgam, Ly6c1, and Ly6g. Pictures were taken using a Biorevo Keyence BZ-9000 microscope with objective from Nikon (Plan Apo 10x/0,45 ∞/0.17 WD 4.0) and the Keyence BZ II Viewer and Analyzer software. Pooled data from 2 of 3 independent experiments are shown. For statistical analysis, the Mann-Whitney test was performed. Results are shown as mean ± SD. *$P < .05$.

It is important to emphasize that in our study the repeated application of ITE alone did not show any adverse effects in any of our experiments. Thus, this study does not question the great therapeutic potential of nontoxic natural Ahr ligands as potent immunosuppressive drugs. In particular, the specific targeting of ITE to antigen-presenting dendritic cells, as has been achieved in vivo via nanoparticles,[22] seems to be a promising approach for a safe and
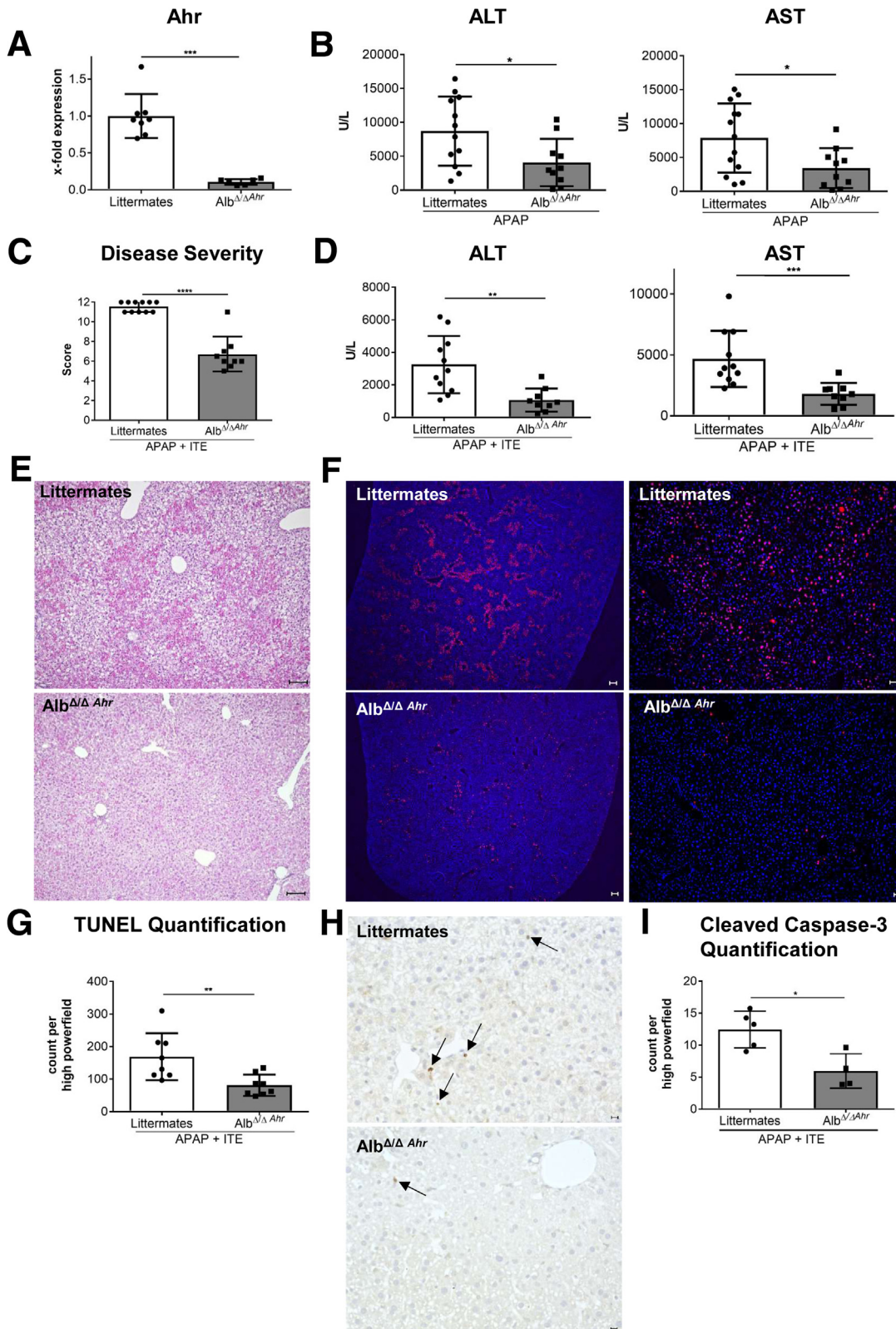
targeted therapeutic intervention in inflammatory diseases. Recently, ITE has also been suggested as an antifibrotic regimen in liver fibrogenesis via inhibition of hepatic stellate cell (HSC) activity. In CCl4-induced liver fibrosis, making use of conditional knockout mice lacking Ahr specifically in HSCs, hepatocytes, or Kupffer cells, it was shown that the protective effect of Ahr activity was dependent on Ahr in HSCs, whereas Ahr was dispensable in hepatocytes or Kupffer cells.[28] Yet, our data indicate that caution should be used when Ahr ligands are used untargeted in combination with APAP intake. Of note, already at therapeutic APAP doses approved for application in humans, combined treatment with ITE at a published therapeutic and nontoxic dose,[29] induced significant serum transaminase elevations and significant hepatocellular cell death (Figure 7). By the same token, even at low dose (ie, one-tenth of the published therapeutic dose)[22–24] ITE-mediated Ahr activation caused significant aggravation of APAP hepatotoxicity, further suggesting a possible clinical relevance of the Ahr pathway in hyperacute APAP-induced liver injury (Figure 7).

Notably, although sex differences in the general sensitivity toward APAP have been described,[25] the observed detrimental effect of Ahr activation on APAP hepatotoxicity was similar in female and male mice (Figure 9).

Taken together, our findings indicate that Ahr activation in hepatocytes sensitizes to APAP-induced acute liver failure by fueling the accumulation of toxic APAP metabolites. Thus, the variable exposure of hepatocytes to nontoxic dietary or microbial Ahr ligands might explain individual sensitivity to APAP-induced acute liver injury. Moreover, our findings strongly advise against therapeutic coadministration of Ahr ligands together with APAP.

Materials and Methods
Animals
We obtained $Ahr^{tm3.1Bra}$/J and $Lyz2^{tm1(cre)Ifo}$/J as a kind gift from Francisco J. Quintana (Harvard Medical School). The Alb-Cre line (B6.Cg-$Speer6$-$ps1^{Tg(Alb-cre)21Mgn}$/J) was obtained from the Jackson Laboratory (Bar Harbor, ME). The Ahr fx mice were bred with the 2 Cre-lines as heterozygotes, producing both Ahr-deficient and Ahr-proficient offspring. Mice were bred and housed under specific pathogen-free-conditions in the animal facility of the University Medical Center Hamburg-Eppendorf in a 12-hour light/dark cycle in individually ventilated cages receiving standard chow. For experiments, sex-matched (either male or female, as indicated in the figure legends) 6- to 9-week-old wild-type mice, $Alb^{\Delta/\Delta Ahr}$ conditional knockout mice lacking Ahr specifically in hepatocytes (B6.FVB(129)-Tg(Alb1-cre) $Ahr^{tm3.1Bra}$), or $LysM^{\Delta/\Delta Ahr}$ conditional knockout mice lacking Ahr specifically in myeloid cells (B6.129P2-Lyz2tm1(cre) $Ahr^{tm3.1Bra}$), and their littermates with functional Ahr (all on C57BL/6 background) were used. Humane endpoints were applied to minimize any harm according to the Guide for the Care and Use of Laboratory Animals (National Institutes of Health publication 86-23, revised 1985). All animal experiments were conducted in accordance with the governmental and institutional guidelines and were approved by the Behörde für Gesundheit und Verbraucherschutz, Fachbereich Veterinärwesen of the State of Hamburg, Germany.

Induction of Acetaminophen-Induced Liver Injury and ITE or FICZ Treatment
Prior to the intraperitoneal injection of 0, 50, 100, 205, or 350 mg/kg APAP (A7085; Sigma-Aldrich, St Louis, MO) (human equivalent doses: 0, 4.1, 8.1, 16.6, or 28.4 mg/kg according to Reagan-Shaw et al),[21] mice were injected intraperitoneally for 2 consecutive days with the reported therapeutic dose of 200-μg ITE or one-third (67 μg) or one-tenth (20 μg) thereof (1803, Tocris Bioscience, Bristol, United Kingdom),[29] or 1-μg FICZ (BML-GR206; Enzo Life Science, Vienna, Austria)[30] or vehicle (corn oil, C8267; Sigma-Aldrich). Sixteen hours before APAP injection, mice were fasted in order to reduce and equilibrate GSH levels. The disease severity was scored for 4 categories, each with 4 grades: eyes open (0) to closed (3), fur straight (0) to scrubby (3), breathing normal (0) to gasping (3), and mobility normal (0) to impaired (3). Liver tissue and blood were collected 0.5, 4, or 8 hours post-APAP treatment. All interventions were done during the light cycle.

Analysis of Serum Transaminases
As a measure of liver damage, ALT and AST serum levels were determined at the Institute of Experimental Immunology and Hepatology, University Medical Centre Hamburg-Eppendorf, using a COBAS Mira System (Roche Diagnostic, Mannheim, Germany).

Analysis of GSH Levels
Concentrations of total GSH levels were measured at the Leibniz Research Centre for Working Environment and Human Factors (Dortmund, Germany) in liver tissue

---

Figure 5. (*See previous page*). **Ahr activation in hepatocytes is responsible for ITE-mediated induction of hyperacute APAP hepatotoxicity.** (*A*) Quantitative polymerase chain reaction–based verification of efficient Ahr knockdown in hepatocytes of female $Alb^{\Delta/\Delta Ahr}$ mice as compared with littermate control mice (n = 6–8). (*B*) Female $Alb^{\Delta/\Delta Ahr}$ mice or their littermates were treated with APAP alone and serum transaminases 8h post treatment were measured (n = 10–12). (*C–J*) Female $Alb^{\Delta/\Delta Ahr}$ mice (n = 9) or littermate control mice (n = 11) were treated with ITE + APAP and analyzed 4h post-APAP treatment. (*C*) Disease severity, (*D*) serum transaminases, (*E*) H&E staining (scale bar = 100 μm), (*F*, *G*) TUNEL staining of dead hepatocytes (red, scale bar = 200 μm [left panels], 50 μm [right panels]) and (*H–I*) analysis of the apoptosis marker cleaved caspase-3 revealed that $Alb^{\Delta/\Delta Ahr}$ mice were protected from ITE-induced hyperacute APAP hepatotoxicity. Pictures were taken using a Biorevo Keyence BZ-9000 microscope (Keyence) with objective from Nikon (Plan Apo 10x/0,45 ∞/0.17 WD 4.0) and the Keyence BZ II Viewer and Analyzer software. Scale bar = 50 μm. Pooled data of 2 of 3 independent experiments are shown. For statistical analysis, the Mann-Whitney test was applied. Results are shown as mean ± SD. **$P < .01$, ***$P < .001$, ****$P < .0001$.
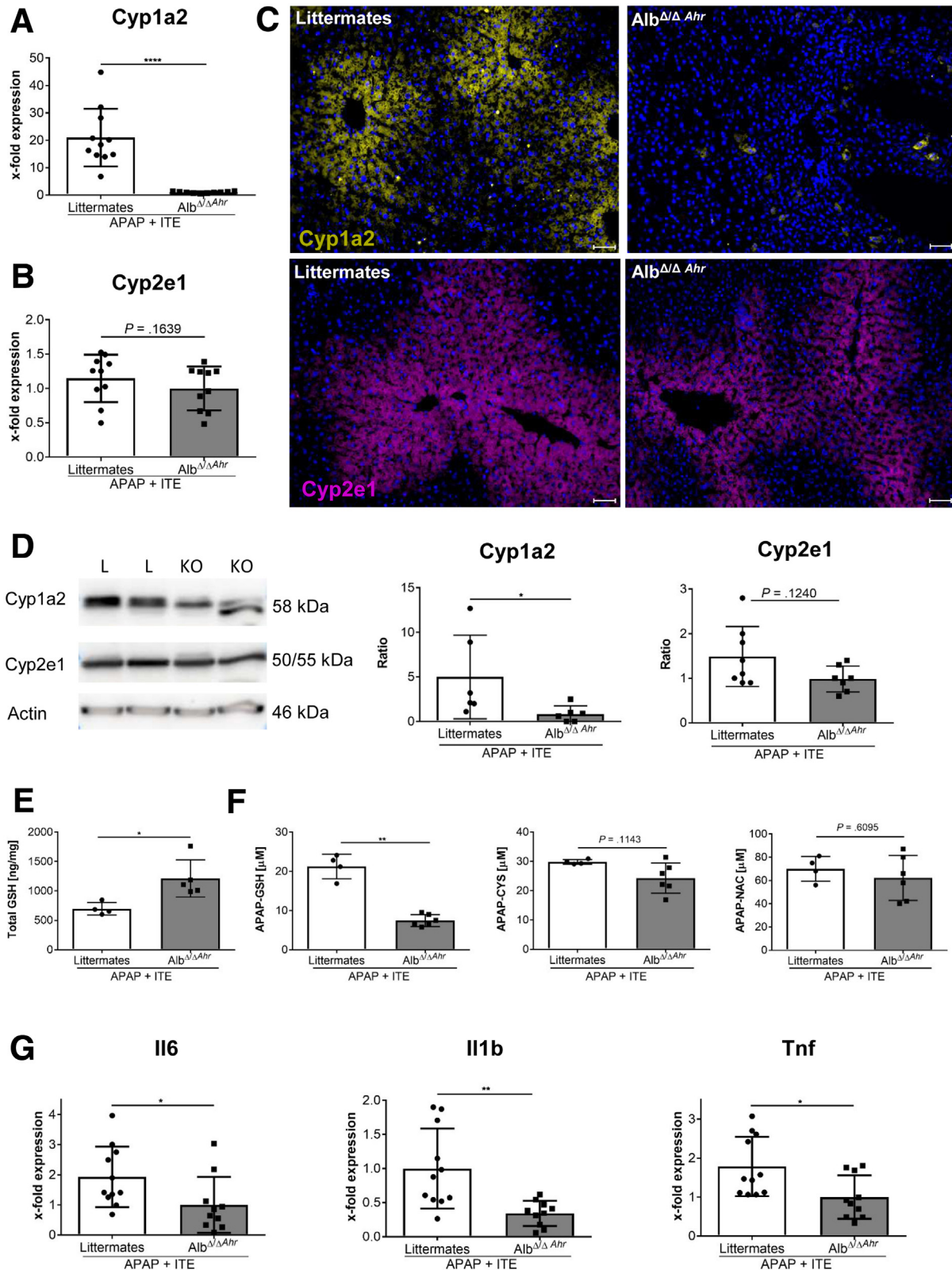
Figure 6. Hyperacute APAP-induced liver injury by Ahr activation in hepatocytes depends on accumulation of toxic APAP adducts. Female Alb$^{\Delta/\Delta Ahr}$ mice and littermate control mice were treated with APAP+ITE (n = 9–11). Expression of the APAP- metabolizing enzymes Cyp1a2 and Cyp2e1 at (A, B) messenger RNA and (C, D) protein level 4 hours post APAP injection. (E) Total GSH levels in liver homogenate and (F) APAP adducts in serum 30 min post APAP injection (n = 4–6). (G) Hepatic expression of the inflammatory cytokines *Il6*, *Il1b* and *Tnf* 4 hours post APAP injection. Pictures were taken using a Biorevo Keyence BZ-9000 microscope with objective from Nikon (Plan Apo 10x/0,45 ∞/0.17 WD 4.0) and the Keyence BZ II Viewer and Analyzer software. Scale bar = 50 μm. Pooled data of 2 of 3 independent experiments are shown. For statistical analysis, the Mann-Whitney test was applied. Results are shown as mean ± SD. **P < .01, ***P < .001, ****P < .0001. KO, Alb$^{\Delta/\Delta Ahr}$; L, littermate.
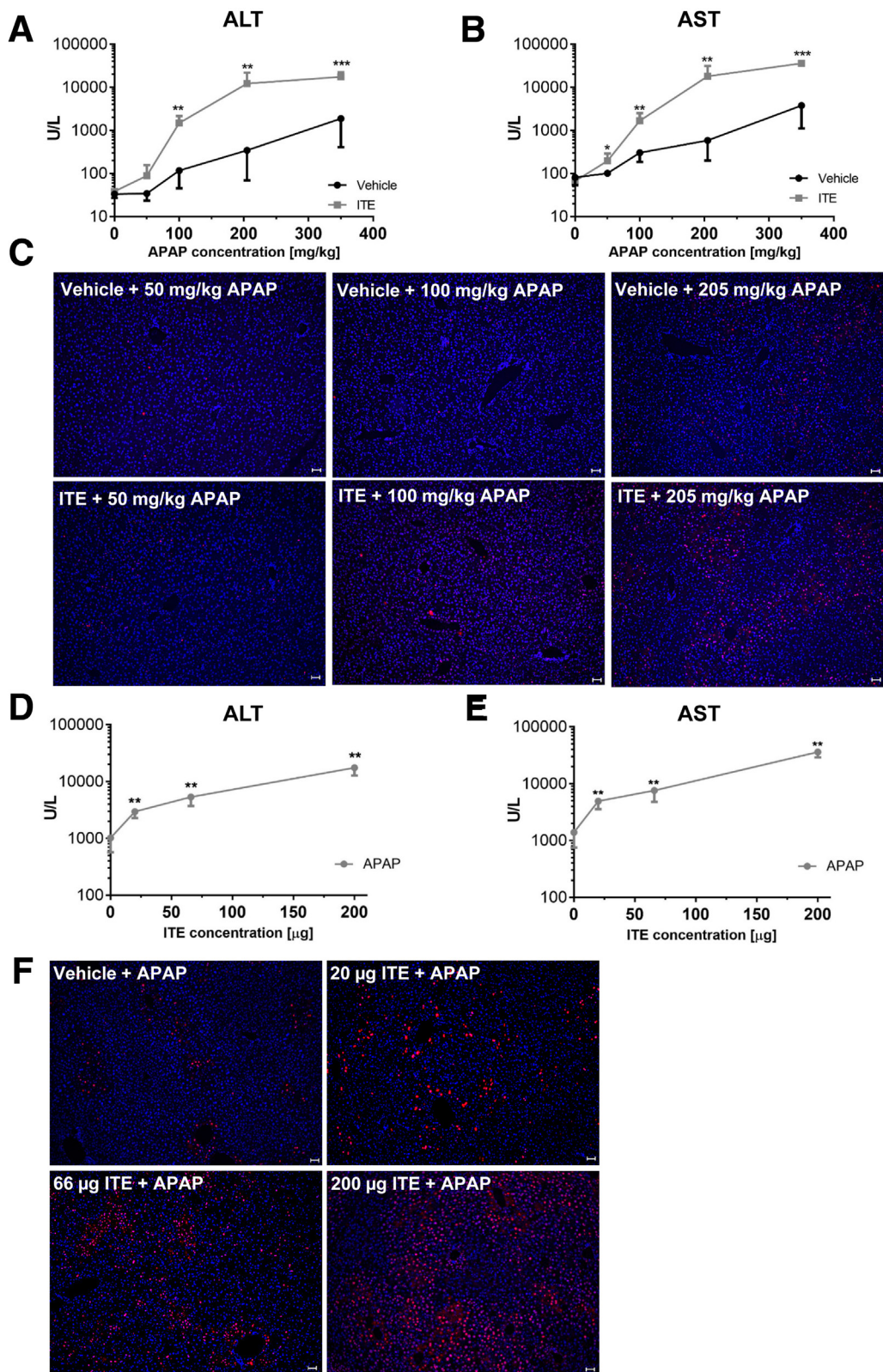
Figure 7. Low-dose APAP in combination with ITE is sufficient to induce hepatocellular damage. (*A–C*) Male wild-type mice were treated with vehicle or ITE + escalating doses of APAP (0, 50, 100, 205, or 350 mg/kg; n = 6 each). (*D–F*) Alternatively, male wild-type mice were treated with vehicle or escalating doses of ITE (0, 20, 67, and 200 μg, n = 6 each) + 350 mg/kg APAP. (*A, D*) ALT and (*B, E*) AST serum levels were measured 4 hours post APAP treatment. (*C, F*) TUNEL staining (red) of representative liver sections. Nuclei are stained in blue. Pictures were taken using a Biorevo Keyence BZ-9000 microscope with objective from Nikon (Plan Apo 10x/0,45 ∞/0.17 WD 4.0) and the Keyence BZ II Viewer and Analyzer software. Scale bar = 50 μm. One representative of 3 independent experiments is shown. For statistical analysis, the Mann-Whitney test was applied. Results are shown as mean $\pm$ SD. **$P < .01$, ***$P < .001$.
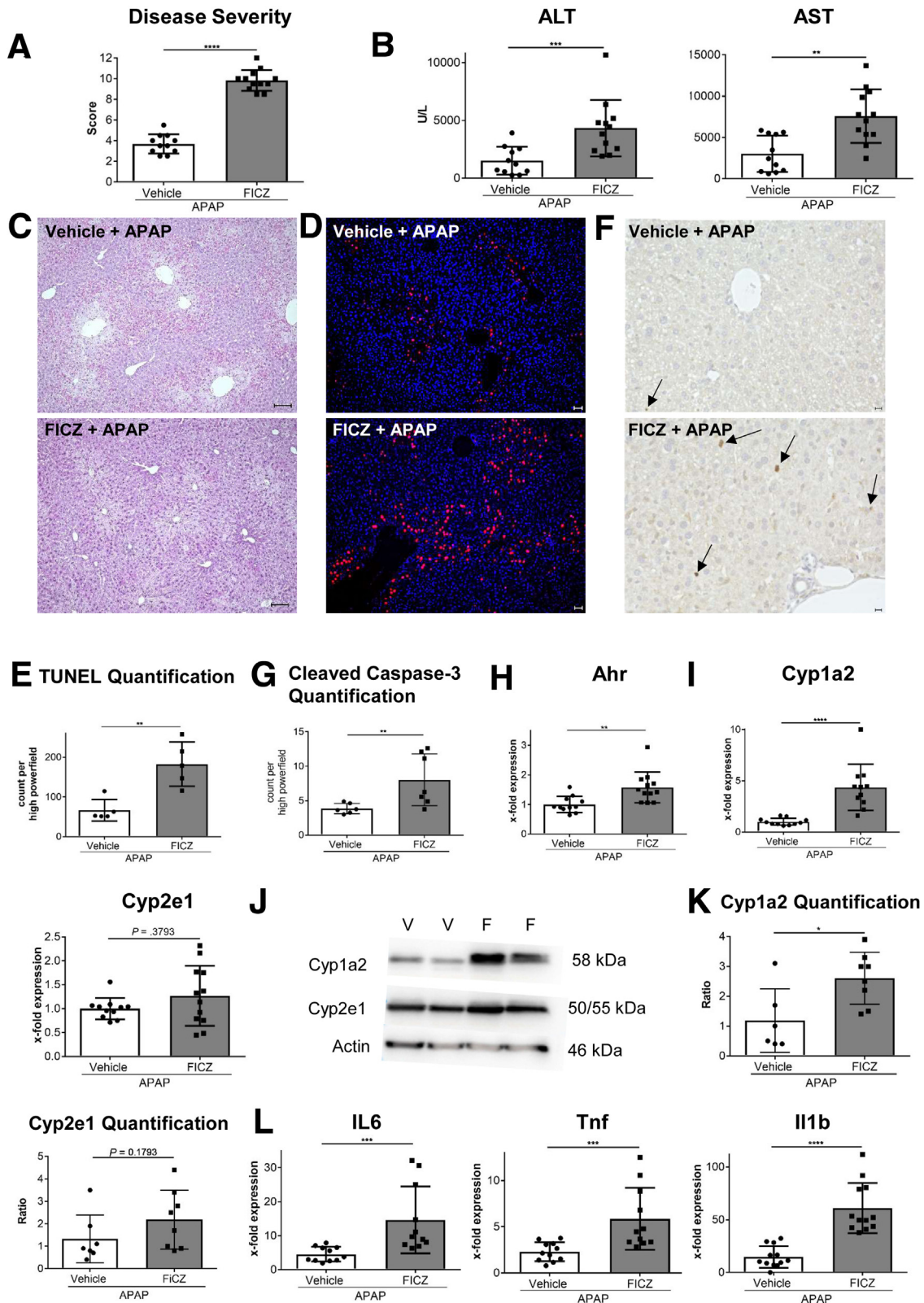
Figure 8. Ahr activation by FICZ induces hyperacute liver damage. Male wild-type mice were treated with vehicle + APAP or FICZ + APAP (n = 11–12). Samples were analyzed 4 hours post-APAP treatment. (*A*) Disease score reflecting general condition, (*B*) serum liver transaminases, and hepatocyte damage as assessed by (*C*) H&E (scale bar = 100 μm), (*D, E*) TUNEL (n = 5 each; red; nuclei are stained in blue) (scale bar = 50 μm), and (*F, G*) cleaved caspase-3 staining. Pictures were taken using a Biorevo Keyence BZ-9000 microscope with objectives from Nikon (Apo 2x/0.10, OFN25 WD 8.5; Plan Apo 10x/0,45 ∞/0.17 WD 4.0) and the Keyence BZ II Viewer and Analyzer software. (*H, I, L*) Hepatic gene expression of *Ahr, Cyp1a2, Cyp2e1* and of the inflammatory cytokines *Il6, Tnf, and Il1b*. (*J, K*) Western blot analysis of Cyp1a2 and Cyp2e1 at protein level. Pooled data of 2 of 3 independent experiments are shown. For statistical analysis, the Mann-Whitney test was performed. Results are shown as mean ± SD. **$P < .01$, ***$P < .001$, ****$P < .0001$. F, FICZ + APAP; V, vehicle + APAP.
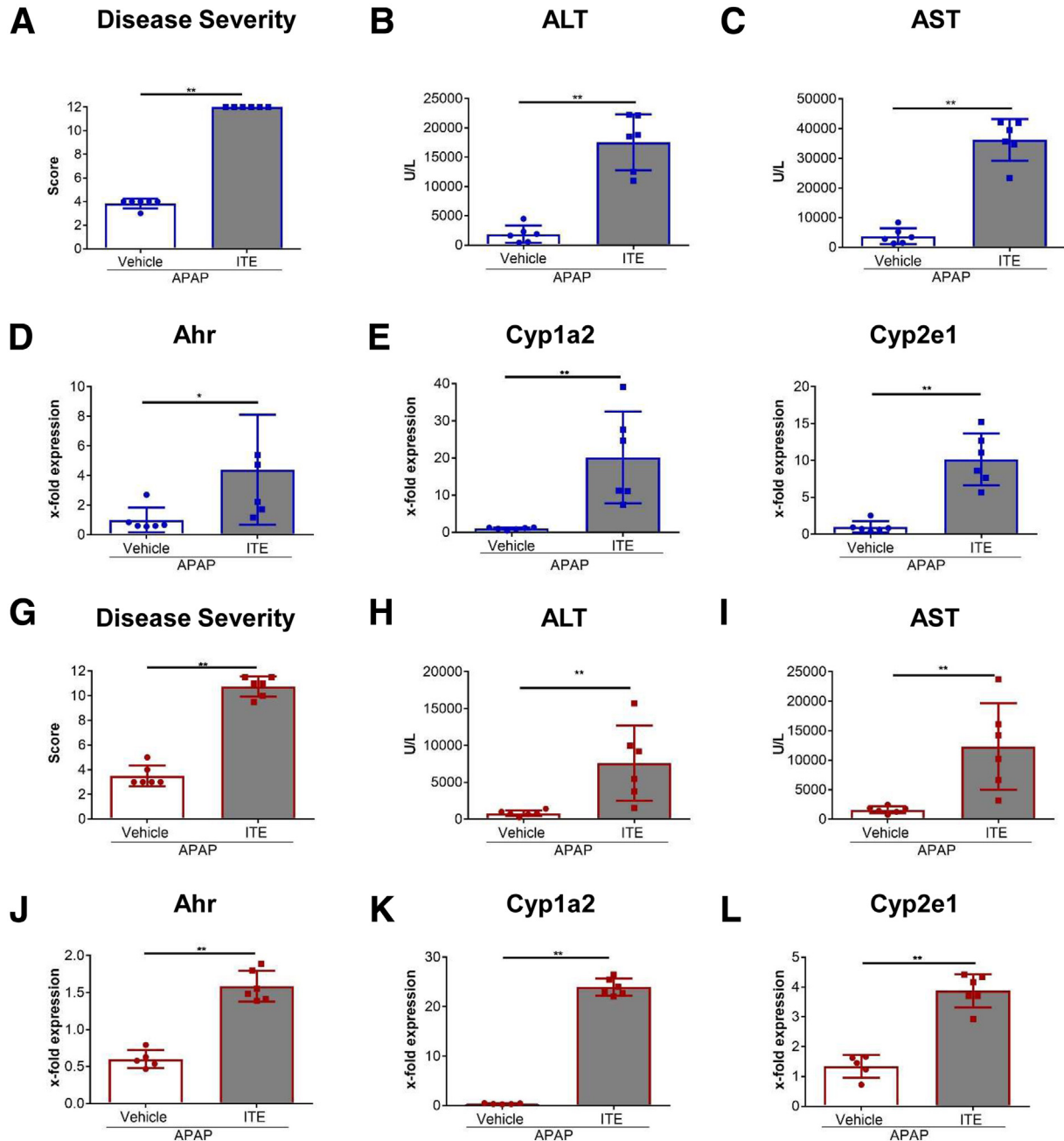
Figure 9. ITE-mediated exacerbation of APAP induced liver injury is similar in both sexes. (*A–F*) Male or (*G–L*) female C57Bl/6 mice (n = 6 each) were injected intraperitoneally on 2 consecutive days with 200 μg ITE or vehicle prior to intraperitoneal injection of 350 mg/kg APAP. (*A, G*) Disease severity, (*B, H*) ALT, and (*C, I*) AST serum levels, and gene expression of *Ahr, Cyp1a2, and Cyp2e1* were analyzed. One representative experiment of 3 independent experiments is shown. For statistical analysis, the Mann-Whitney test was applied. Mean $\pm$ SD are shown. *$P < .05$, **$P < .01$.

homogenate 30 minutes post APAP administration using LC-MS/MS, as described in Sezgin et al.[31]

Analysis of APAP Adducts

Concentrations of APAP adducts (APAP-glutathione, APAP-cysteine, APAP-N-acetylcysteine) were measured at the Center for Mass Spectrometry, Faculty of Chemistry and Chemical Biology, TU Dortmund University (Dortmund, Germany) in blood plasma 30 minutes post APAP treatment

using high-performance liquid chromatography tandem mass spectrometry, as described in Sezgin et al.[31]

Liver Histology and Detection of Cell Death and Apoptosis

Livers were perfused in situ with phosphate-buffered saline, fixed in 4% formalin, and embedded in paraffin. Liver sections were then stained with hematoxylin and eosin. Alternatively, for the detection of dead cells, TUNEL

was performed with the in situ cell death detection Kit, TMR red (12156792910; Roche, Zurich, Switzerland) according to the manufacturer's instructions. Nuclei were counterstained with Hoechst 33258 nuclear dye (H3569; Thermo Fisher Scientific, Waltham, MA). For determination of apoptotic cells, immunohistochemistry staining of cleaved caspase-3 (Antibody 9661S [Cell Signaling, Danvers, MA], DAB-HRP System K5007 [Dako, Carpinteria, CA]) was performed. Cell death and apoptosis were quantified by single cell point counting using ImageJ Version 1.51q (National Institutes of Health, Bethesda, MD).

Immunofluorescence Staining

Cryo-preserved liver sections were fixed in acetone/methanol and stained with anti-CYP2E1 (HPA009128, polyclonal; Sigma-Aldrich) or anti-CYP1A2 (19936-1-AP, polyclonal, Proteintech, Rosemont, IL) and a secondary AF647-labelled goat anti-rabbit antibody (A21245; Thermo Fisher Scientific). Liver sections were counterstained with Hoechst 33258 nuclear dye (Invitrogen, Carlsbad, CA) and embedded in Dako fluorescence mounting medium (Ref. S3023; Dako). Pictures were taken using a Biorevo Keyence BZ-9000 microscope (Keyence, Osaka, Japan) with objectives from Nikon (Tokyo, Japan) (Apo 2x/0.10, OFN25 WD 8.5; Plan Apo 10x/0,45 ∞/0.17 WD 4.0; Plan Apo 20x/0.75 ∞/0.17 WD 1.6) and the Keyence BZ II Viewer and Analyzer software.

Western Blot

Frozen fixed liver tissue was lysed with T-PER Tissue Protein Extraction Reagent (78510; Thermo Fisher Scientific) and proteinase inhibitors. The total protein concentration was measured using Pierce BCA Protein Assay Kit (23225; Thermo Fisher Scientific) and equal amounts of 20 μg protein or 5 μL of PageRuler Plus Prestained Protein Ladder (26619; Thermo Fisher Scientific) were separated by 12% sodium dodecyl sulfate polyacrylamide gel electrophoresis and transferred to nitrocellulose blotting membranes (10600002; GE Healthcare Life Sciences, Chicago, IL). Afterward, the membranes were blocked 1 hour at room temperature with 5% dry fat-free milk in Tris-buffered saline containing 0.05% Tween 20 (P1379; Sigma-Aldrich) and incubated in combination with the primary antibodies to Actin (J0711; Santa Cruz Biotechnology, Dallas, TX), CYP2E1 (HPA009128, polyclonal; Sigma-Aldrich) or CYP1A2 (19936-1-AP, polyclonal; Proteintech) in 5% dry fat-free milk in Tris-buffered saline containing 0.05% Tween 20 overnight at 4°C, or with secondary rabbit horseradish peroxidase–conjugated antibody at room temperature for 1 hour, respectively. Protein-antibody complexes were detected using Super-Signal West Dura Extended Duration Substrate (34076; Thermo Fisher Scientific) and visualized by Fusion FX6 system (Vilber, Eberhardzell, Germany) and Fusion FX6 Software (Vilber). The protein bands from at least 3 independent blots were quantified by average ratios of integral optical density and normalized to the housekeeper control actin.

Flow Cytometric Analysis of Liver NPCs

Nonparenchymal cells (NPCs) were isolated as described previously.[32] Briefly, livers were perfused with phosphate-buffered saline in situ and homogenized, and the obtained single cells were subjected to density gradient centrifugation (36% Optiprep; Sigma-Aldrich). Afterward, the harvested NPCs were stained with Pacific Orange succinimidyl ester (Thermo Fisher Scientific) for dead cell exclusion and with fluorochrome-labelled antibodies to CD45 (110724), CD11b (101262), Ly6C (175619), and Ly6G (127608) (all from BioLegend, San Diego, CA). Analysis was performed using a BD FACS LSR II (BD Biosciences, Franklin Lakes, NJ) and FlowJo software (version 10.5.0; BD Biosciences).

Confirmation of Ahr Deficiency in Knockout Cells

In order to verify Ahr knockout in hepatic myeloid cells of LysM$^{\Delta/\Delta Ahr}$ mice, F4/80+ cells were magnetically separated from liver NPCs of LysM$^{\Delta/\Delta Ahr}$ mice or their littermates using MACS technology (F4/80 antibody, anti-PE Microbeads). Subsequently, the obtained liver macrophages were subjected to Ahr gene expression analysis. Similarly, Ahr knockout in hepatocytes of Alb$^{\Delta/\Delta Ahr}$ mice was confirmed by Ahr gene expression analysis.

Gene Expression Analysis

RNA was isolated from whole liver tissue or primary liver macrophages using the reagent NucleoSpin RNA Kit (Macherey-Nagel, Düren, Germany) and further transcribed into complementary DNA using the High Capacity cDNA Reverse Transcription Kit (Thermo Fisher Scientific). Real time quantitative polymerase chain reaction was performed on a ViiA7 System (Thermo Fisher Scientific). The following TaqMan primers were used: Ahr- Mm00478930_m1, Cyp1a2- Mm00487224_m1, Cyp2e1- Mm00491127_m1, Itgam - Mm00434455_m1, Ly6c1- Mm03009946_m1, Ly6g- Mm04934123_m1, Il6- Mm00446190_m1, Tnf- Mm00443258_m1, Ccl2- Mm00441242_m1, Il18- Mm00434226_m1, Il1b- Mm00434228_m1, Hprt - Mm01545399_m1 (all Thermo Fisher Scientific). Gene expression was normalized to the house keeping gene Hprt and calculated by the 2$^{-\Delta\Delta Ct}$ method.

Statistical Analysis

Data analysis was performed with GraphPad Prism Version 6 (GraphPad Software, San Diego, CA). For 2 group comparisons, the nonparametric Mann-Whitney test was used. For multiple comparisons, a 1-way analysis of variance followed by Tukey's multiple comparisons test was applied. For survival curves, 2 groups were compared with log-rank (Mantel-Cox test) and Gehan-Breslow-Wilcoxon test. All results are shown as mean ± SD. Levels of significance are indicated as $P < .05$, $P < .01$, $P < .001$, and $P < .0001$.

References

1. Yoon E, Babar A, Choudhary M, Kutner M, Pyrsopoulos N. Acetaminophen-induced hepatotoxicity:

a comprehensive update. J Clin Transl Hepatol 2016;
4:131–142.

2. Zaher H, Buters JT, Ward JM, Bruno MK, Lucas AM,
Stern ST, Cohen SD, Gonzalez FJ. Protection against
acetaminophen toxicity in CYP1A2 and CYP2E1 double-
null mice. Toxicol Appl Pharmacol 1998;152:193–199.

3. Herndon CM, Dankenbring DM. Patient perception and
knowledge of acetaminophen in a large family medicine
service. J Pain Palliat Care Pharmacother 2014;
28:109–116.

4. Heard K, Green JL, Anderson V, Bucher-Bartelson B,
Dart RC. A randomized, placebo-controlled trial to
determine the course of aminotransferase elevation
during prolonged acetaminophen administration. BMC
Pharmacol Toxicol 2014;15:39.

5. Gulmez SE, Larrey D, Pageaux GP, Lignot S, Lassalle R,
Jové J, Gatta A, McCormick PA, Metselaar HJ,
Monteiro E, Thorburn D, Bernal W, Zouboulis-Vafiadis I,
de Vries C, Perez-Gutthann S, Sturkenboom M,
Bénichou J, Montastruc JL, Horsmans Y, Salvo F,
Hamoud F, Micon S, Droz-Perroteau C, Blin P, Moore N.
Transplantation for acute liver failure in patients exposed
to NSAIDs or paracetamol (acetaminophen): the multi-
national case-population SALT study. Drug Saf 2013;
36:135–144.

6. Caparrotta TM, Antoine DJ, Dear JW. Are some people at
increased risk of paracetamol-induced liver injury? A
critical review of the literature. Eur J Clin Pharmacol
2018;74:147–160.

7. Mimura J, Fujii-Kuriyama Y. Functional role of Ahr in the
expression of toxic effects by TCDD. Biochim Biophys
Acta 2003;1619:263–268.

8. Esser C, Rannug A. The aryl hydrocarbon receptor in
barrier organ physiology, immunology, and toxicology.
Pharmacol Rev 2015;67:259–279.

9. Rothhammer V, Quintana FJ. The aryl hydrocarbon re-
ceptor: an environmental sensor integrating immune re-
sponses in health and disease. Nat Rev Immunol 2019;
19:184–197.

10. Krishnan S, Ding Y, Saedi N, Choi M, Sridharan GV,
Sherr DH, Yarmush ML, Alaniz RC, Jayaraman A, Lee K.
Gut microbiota-derived tryptophan metabolites modu-
late inflammatory response in hepatocytes and macro-
phages. Cell Rep 2018;23:1099–1111.

11. Cho S, Tripathi A, Chlipala G, Green S, Lee H, Chang EB,
Jeong H. Fructose diet alleviates acetaminophen-
induced hepatotoxicity in mice. PLoS One 2017;12:
e0182977.

12. Gong S, Lan T, Zeng L, Luo H, Yang X, Li N, Chen X,
Liu Z, Li R, Win S, Liu S, Zhou H, Schnabl B, Jiang Y,
Kaplowitz N, Chen P. Gut microbiota mediates diurnal
variation of acetaminophen induced acute liver injury in
mice. J Hepatol 2018;69:51–59.

13. Xu S, Liu J, Shi J, Wang Z, Ji L. 2,3,4',5-
tetrahydroxystilbene-2-O-β-D-glucoside exacerbates
acetaminophen-induced hepatotoxicity by inducing he-
patic expression of CYP2E1, CYP3A4 and CYP1A2. Sci
Rep 2017;7:16511.

14. Chowdhary V, Teng KY, Thakral S, Zhang B, Lin CH,
Wani N, Bruschweiler-Li L, Zhang X, James L, Yang D,

Junge N, Brüschweiler R, Lee WM, Ghoshal K. miRNA-
122 protects mice and human hepatocytes from acet-
aminophen toxicity by regulating cytochrome P450 family
1 subfamily A member 2 and family 2 subfamily E member
1 expression. Am J Pathol 2017;187:2758–2774.

15. Nebert DW, Dalton TP, Okey AB, Gonzalez FJ. Role of
aryl hydrocarbon receptor-mediated induction of the
CYP1 enzymes in environmental toxicity and cancer.
J Biol Chem 2004;279:23847–23850.

16. Shinde R, McGaha TL. The aryl hydrocarbon receptor:
connecting immunity to the microenvironment. Trends
Immunol 2018;39:1005–1020.

17. Mossanen JC, Krenkel O, Ergen C, Govaere O, Liepelt A,
Puengel T, Heymann F, Kalthoff S, Lefebvre E,
Eulberg D, Luedde T, Marx G, Strassburg CP,
Roskams T, Trautwein C, Tacke F. Chemokine (C-C
motif) receptor 2-positive monocytes aggravate the early
phase of acetaminophen-induced acute liver injury.
Hepatology 2016;64:1667–1682.

18. Krenkel O, Mossanen JC, Tacke F. Immune mechanisms
in acetaminophen-induced acute liver failure. Hep-
atobiliary Surg Nutr 2014;3:331–343.

19. Walisser JA, Glover E, Pande K, Liss AL, Bradfield CA.
Aryl hydrocarbon receptor-dependent liver develop-
ment and hepatotoxicity are mediated by different cell
types. Proc Natl Acad Sci U S A 2005;
102:17858–17863.

20. Goudot C, Coillard A, Villani AC, Gueguen P, Cros A,
Sarkizova S, Tang-Huau TL, Bohec M, Baulande S,
Hacohen N, Amigorena S, Segura E. Aryl hydrocarbon re-
ceptor controls monocyte differentiation into dendritic cells
versus macrophages. Immunity 2017;47:582–596.e6.

21. Reagan-Shaw S, Nihal M, Ahmad N. Dose translation
from animal to human studies revisited. FASEB J 2008;
22:659–661.

22. Yeste A, Nadeau M, Burns EJ, Weiner HL, Quintana FJ.
Nanoparticle-mediated codelivery of myelin antigen and
a tolerogenic small molecule suppresses experimental
autoimmune encephalomyelitis. Proc Natl Acad Sci U S
A 2012;109:11270–11275.

23. Yeste A, Takenaka MC, Mascanfroni ID, Nadeau M,
Kenison JE, Patel B, Tukpah AM, Babon JA, DeNicola M,
Kent SC, Pozo D, Quintana FJ. Tolerogenic nano-
particles inhibit T cell-mediated autoimmunity through
SOCS2. Sci Signal 2016;9:ra61.

24. Goettel JA, Gandhi R, Kenison JE, Yeste A,
Murugaiyan G, Sambanthamoorthy S, Griffith AE, Patel B,
Shouval DS, Weiner HL, Snapper SB, Quintana FJ. AHR
activation is protective against colitis driven by T cells in
humanized mice. Cell Rep 2016;17:1318–1329.

25. Du K, Williams CD, McGill MR, Jaeschke H. Lower sus-
ceptibility of female mice to acetaminophen hepatotox-
icity: Role of mitochondrial glutathione, oxidant stress
and c-jun N-terminal kinase. Toxicol Appl Pharmacol
2014;281:58–66.

26. Di Meglio P, Duarte JH, Ahlfors H, Owens ND, Li Y,
Villanova F, Tosi I, Hirota K, Nestle FO, Mrowietz U,
Gilchrist MJ, Stockinger B. Activation of the aryl hydro-
carbon receptor dampens the severity of inflammatory
skin conditions. Immunity 2014;40:989–1001.

27. Hammerschmidt-Kamper C, Biljes D, Merches K, Steiner I, Daldrup T, Bol-Schoenmakers M, Pieters RHH, Esser C. Indole-3-carbinol, a plant nutrient and Ahr-Ligand precursor, supports oral tolerance against OVA and improves peanut allergy symptoms in mice. PLoS One 2017;12:e0180321.

28. Yan J, Tung HC, Li S, Niu Y, Garbacz WG, Lu P, Bi Y, Li Y, He J, Xu M, Ren S, Monga SP, Schwabe RF, Yang D, Xie W. Aryl hydrocarbon receptor signaling prevents activation of hepatic stellate cells and liver fibrogenesis in mice. Gastroenterology 2019; 157:793–806.

29. Quintana FJ, Murugaiyan G, Farez MF, Mitsdoerffer M, Tukpah AM, Burns EJ, Weiner HL. An endogenous aryl hydrocarbon receptor ligand acts on dendritic cells and T cells to suppress experimental autoimmune encephalo-myelitis. Proc Natl Acad Sci U S A 2010; 107:20768–20773.

30. Liu Z, Li L, Chen W, Wang Q, Xiao W, Ma Y, Sheng B, Li X, Sun L, Yu M, Yang H. Aryl hydrocarbon receptor activation maintained the intestinal epithelial barrier function through Notch1 dependent signaling pathway. Int J Mol Med 2018;41:1560–1572.

31. Sezgin S, Hassan R, Zühlke S, Kuepfer L, Hengstler JG, Spiteller M, Ghallab A. Spatio-temporal visualization of the distribution of acetaminophen as well as its metab-olites and adducts in mouse livers by MALDI MSI. Arch Toxicol 2018;92:2963–2977.

32. Glaser F, John C, Engel B, Höh B, Weidemann S, Dieckhoff J, Stein S, Becker N, Casar C, Schuran FA, Wieschendorf B, Preti M, Jessen F, Franke A, Carambia A, Lohse AW, Ittrich H, Herkel J, Heeren J, Schramm C, Schwinge D. Liver infiltrating T cells regu-late bile acid metabolism in experimental cholangitis. J Hepatol 2019;71:783–792.

Correspondence
Address correspondence to: Dr. rer. nat. Antonella Carambia, Department of Medicine I, University Medical Center Hamburg-Eppendorf, Martinistraße 52, 20246 Hamburg, Germany. e-mail: a.carambia@uke.de; fax: +49 40 7410 58014.